Bhattacharjee, G., and Baker, J. W. (2023). "Using global variance-based sensitivity analysis to prioritise bridge retrofits in a regional road network subject to seismic hazard." *Structure and Infrastructure Engineering* 19(2), 164-177. https://doi.org/10.1080/15732479.2021.1931892

Using global variance-based sensitivity analysis to prioritise bridge retrofits in a regional road network subject to seismic hazard

Gitanjali Bhattacharjee, Jack W. Baker

Abstract

This paper presents a novel method for prioritising bridge retrofits within a regional road network subject to uncertain seismic hazard, using a technique that accounts for network performance while avoiding the combinatoric computational costs of exhaustive searches. Using global variance-based sensitivity analysis, a probabilistic ranking of bridges is determined according to how much their retrofit statuses influence the expected cost of the road network disruption. Bridges' total-order sensitivity (Sobol') indices are estimated with respect to the expected cost using the hybrid-point Monte Carlo approximation method. A bridge's total-order Sobol' index measures how much its retrofit status influences the variance of the expected cost of the road network performance and accounts for the effect of its interactions with other bridges' retrofit states. For 71 highway bridges in San Francisco, a retrofit strategy based on bridges' total-order Sobol' indices outperforms other heuristic strategies. The proposed method remains computationally tractable while accounting for the probabilistic nature of the seismic hazard, the uniqueness of individual bridges, network effects, and decision-makers' priorities. Because this method leverages existing risk assessment tools and models without imposing further assumptions, it should be extensible to other types of networks under different types of hazards and to other decision variables.

Keywords: transportation networks, sensitivity analysis, risk management, retrofitting, earthquake engineering, decision making

1 Introduction

This paper presents a novel method for prioritising bridge retrofits within a regional road network subject to uncertain seismic hazard, using a technique that accounts for network effects and disruptions while avoiding the combinatoric computational costs of exhaustive searches. This method uses global variance-based sensitivity analysis (SA) to compute a probabilistic ranking of bridges according to how much their retrofit status influences the decision variable of interest. The proposed method is demonstrated on a network of $B = 71$ unique bridges in the San Francisco Bay Area for two decision variables of interest: (1) the expected cost of the road network performance (2) the ratio of the cost of bridge seismic retrofits to the expected cost of the road network performance. The performance of the

proposed method is compared to that of other heuristic retrofit prioritisation strategies.

The key contribution of this research is in providing a flexible decision-support tool with which to manage risks to complex, real-world networks. The proposed SA-based retrofit prioritisation method builds upon existing event-based probabilistic hazard frameworks that include a set of potential seismic scenarios, described by magnitudes and occurrence rates established using seismic risk assessment procedures. This method leverages existing tools and models without imposing further assumptions – it should therefore be extensible to other types of networks under different types of hazards and with consideration given to different decision-makers' priorities.

This paper is organised as follows: Section 2 reviews pre-earthquake bridge seismic retrofit prioritisation strategies, Section 3 introduces the proposed bridge retrofit prioritisation method, Section 4 presents an example application to illustrate the proposed method and compare its performance with that of other heuristic retrofit strategies, Section 5 provides further discussion of how to implement the proposed method, and Section 6 gives conclusions.

2 Background

Road networks are lifelines and play an important role in everyday life as well as in response and community recovery after an earthquake, as they enable repairs to other lifelines (Frangopol & Bocchini, 2012). Bridges are often the most fragile components of road networks subject to seismic hazard, and bridge damage due to earthquakes can be costly (e.g., Gordon et al., 1998). Retrofitting is an effective method of mitigating the risk of bridge damage due to earthquakes (e.g., Giovinazzi et al., 2011). Deciding which bridges within a large road network to retrofit to meet a particular system performance objective remains a challenging problem, due to the size and complexity of the road network, the large number of possible retrofit combinations, and the number of earthquake rupture scenarios that must be considered to describe the regional seismic hazard (Gomez & Baker, 2019).

Approaches to pre-earthquake bridge seismic retrofit prioritisation can be broadly categorised as heuristic or optimization-based. Heuristic approaches prioritise bridges for retrofit according to an importance measure. Characteristic-based, conditional, reliability-based, and network topology-based importance measures constitute four classes of commonly used importance measures. Characteristic-based importance measures are the least computationally expensive, as they rely only on information about an individual bridge's particular characteristics, such as the average number of vehicles that pass over it in a day (e.g., Buckle et al., 2006; Miller, 2014). More sophisticated characteristic-based importance measures like the indices method proposed by Buckle et al. (2006) combine multiple criteria, including bridges' structural characteristics, socioeconomic importance, and site seismic characteristics (Buckle et al., 2006; Sims, 2000). Buckle et al. (2006) also proposed the expected damage method, which involves assessing the severity of the expected damage of each bridge in the road network for a single earthquake, and the seismic risk assessment method, which involves estimating the effect on system performance of bridge damage for

a given hazard level. Rokneddin (2013) extends the expected damage method of Buckle et al. (2006) to account for how bridge fragilities change with time by ranking bridges using time-dependent fragility analysis. These prioritisation methods do not take into account the topology or performance of the road network and assess bridges independently of one another.

Conditional importance measures quantify the probability that a system component has failed given that the system as a whole has failed, and are generally applicable to infrastructure network components (Rokneddin, 2013; Song & Kiureghian, 2005). They allow the analyst to include some measure of network performance when assessing the importance of individual components in the network. Basic conditional importance measures include the risk achievement worth (RAW), risk reduction worth (RRW), and boundary probability (BP), each of which estimates the sensitivity of a system's failure probability to the states of its constituent components – when a component is damaged (RAW), when a component is invulnerable (RRW), and when a component is upgraded (BP) (Dutuit & Rauzy, 2015; Song & Kiureghian, 2005). Barker et al. (2013) propose two variants of the RAW and RRW that incorporate a measure of network resilience. RAW, RRW, and BP do not account for the vulnerability of the network components to damage, nor any dependencies that might exist between them, and are computed in a deterministic setting, thus neglecting key features of an infrastructure network (Borgonovo & Plischke, 2016; Frangopol & Bocchini, 2012; Miller, 2014; Song & Kiureghian, 2005). Because they require estimation of both system and component failure probabilities, conditional importance measures may be expensive to compute compared to other importance measures (Rokneddin, 2013; Song & Kiureghian, 2005). Miller (2014) proposes a composite importance measure to classify bridges for preliminary retrofit screening according to how frequently they appear in damage maps that result in high losses in network performance. The composite importance measure is probabilistic and can capture non-linearities in the road network performance that result from simultaneous bridge failures .

Moghtaderi-Zadeh and Kiureghian (1983) develop a geometric method for efficiently identifying "critical" components (whether nodes or edges) of large lifeline networks exposed to seismic hazard. Small changes in the strength of these critical components produce significant changes to the network's reliability (Moghtaderi-Zadeh & Kiureghian, 1983). M. Liu and Frangopol (2005) formulate the reliability importance factor of a bridge in a road network as the ratio of the change in reliability of the road network when a bridge's reliability changes to that of the change in the reliability of the individual bridge. Their formulation is intended to prioritise bridges for maintenance rather than retrofit and does not take into account seismic hazard (M. Liu & Frangopol, 2005). The random forests importance measure proposed by Rokneddin (2013) accounts for bridges' vulnerability and their roles in the larger road network and results in a probabilistic ranking, but does not account for the performance of the road network in terms of congestion. Another approach to quantify the importance of different bridges in a road network is to adapt metrics from classic network analysis, such as bridges' betweenness centrality (e.g., Rokneddin et al., 2013). Rokneddin (2013) also proposes BridgeRank, which combines a bridge's topological importance with its fragility to determine its importance within the road network. BridgeRank does not

account for network performance or multiple earthquake scenarios, though it does consider the network topology (Rokneddin, 2013).

The computational tractability of importance measures for large infrastructure networks comes at the expense of other desirable characteristics, among them that an importance measure should account for the likelihood of bridge damage in different scenarios, the performance of the road network, and the effects of multiple bridge failures. Most of the importance measures discussed above sacrifice at least one of these qualities. Furthermore, most importance measures account only for the effects of bridge damage and neglect to model the effects of bridge retrofits; none incorporate budgetary constraints.

Optimisation-based approaches select a subset of bridges within a road network to retrofit such that a user-defined objective is met and guarantee a solution with some degree of optimality. Two-stage stochastic programs are popular in infrastructure risk management literature (Grass & Fischer, 2016) and allow for simultaneous consideration of pre- and post-earthquake decisions, i.e., retrofit and repair, as well as budgetary constraints (Barbarasoglu & Arda, 2004; Fan et al., 2010; Gomez & Baker, 2019; C. Liu et al., 2009; Miller-Hooks et al., 2012; Peeta et al., 2010). Optimisation-based approaches also offer flexibility in terms of decision-makers' priorities: objective functions include measures of road network sustainability (Dong et al., 2014), reliability (Zhang & Wang, 2016), resilience (Miller-Hooks et al., 2012), maximum network flow (Chang et al., 2012), and aggregate retrofit and repair costs (Gomez & Baker, 2019). Optimisation-based approaches have been demonstrated on smaller systems, but application to large networks remains challenging. Most have been applied to networks with fewer than 20 bridges (e.g., Dong et al., 2014; Fan et al., 2010; Peeta et al., 2010), with some notable exceptions: Chang et al. (2012) consider 616 bridges of the same structural type, and Gomez and Baker (2019) consider 65 unique bridges. Common simplifications include considering one earthquake scenario rather than conducting a probabilistic analysis (e.g., Chang et al., 2012; Miller-Hooks et al., 2012; Zhang & Wang, 2016), modelling bridges as having identical structural characteristics (e.g., Chang et al., 2012), assuming that retrofitted bridges cannot be damaged (e.g., C. Liu et al., 2009), or assuming that bridges fail independently of one another (e.g., Peeta et al., 2010).

3 Methods

3.1 Global variance-based sensitivity analysis

Saltelli et al. (2004) define sensitivity analysis as "the study of how the uncertainty in the output of a model ... can be apportioned to different sources of uncertainty in the model input". Local (or deterministic) SA is performed around a particular point of interest in the model input space, in contrast to global (or probabilistic) SA, which considers the entire model input space (Borgonovo & Plischke, 2016; Saltelli et al., 2004). A global variance-based SA aims to attribute the variability in a scalar output quantity of interest q to variability in the n_B input quantities $\boldsymbol{f} = [f_1, f_2, ...f_{n_B}]$ given some function (not necessarily expressible in closed form) relating the two, $g(\boldsymbol{f}) = q$. Equation (1) gives the

basic form of a global SA problem.

$$\boldsymbol{f} \rightarrow g(\boldsymbol{f}) \rightarrow q \tag{1}$$

Sensitivity indices quantify the portion of the variability of q associated with an input $f_b, b \in \{1, \ldots, n_B\}$. Computing the sensitivity indices of a set of inputs requires treating each input as a random variable by assigning it a distribution. The portion of the variance of q that can be attributed to an input f_b is bounded by the first- and total-order sensitivity indices of f_b. The first-order sensitivity index, given in Equation (2), quantifies how much of the variance in q can be attributed solely to variance in f_b. In Equation (2), $\{b\}$ denotes a set containing only the input variable indexed by b.

$$\underline{S}_b^2 = \frac{V[\mathbb{E}[q|f_{\{b\}}]]}{V[q]} \tag{2}$$

A second-order sensitivity index quantifies how much of the variance in q can be attributed to variance in f_b and a second input, denoted f_c, including interactions between those two variables. An interaction is that part of the response of the output q to the values of f_b and f_c "that cannot be expressed as a superposition of effects separately due to" f_b and f_c (Saltelli et al., 2004). The total-order sensitivity index of f_b, given in Equation (3), is the sum of the first- and all higher-order sensitivity indices of f_b. It quantifies how much of the variance in the output quantity q can be attributed to variance in the input quantity f_b and its interactions with all other input variables, denoted by the set $\_\{b\}$.

$$\overline{S}_b^2 = \frac{\mathbb{E}(V[q|f_{\_\{b\}}])}{V[q]} \tag{3}$$

Both the first and total-order index of f_b take values in $[0, 1]$. $\overline{S}_b^2 = 0$ indicates that the input f_b is non-influential – i.e., variability in its value does not contribute to variability in the output. It can therefore be fixed to any value within its distribution without impacting the output variance (Saltelli et al., 2008). Larger indices indicate that the associated inputs are more influential with respect to the output.

3.2 Estimation of total-order Sobol' indices

The total-order sensitivity index in Equation (3) is expensive to compute exactly (Saltelli et al., 2008). Sobol (1993) developed an estimator for the total-order sensitivity index by using a hybrid-point Monte Carlo approximation approach, summarised for a set of input variables and function $g(\boldsymbol{f})$ in Algorithm 1. This estimator is referred to as the total-order Sobol' index.

Equation (4) gives the estimate of the unnormalised total-order Sobol' index for an input variable f_b, where $\boldsymbol{f}_{i,b'} : \boldsymbol{f}'_{i,b}$ denotes the hybrid point, constructed by interleaving elements of the vectors $\boldsymbol{f}_{i,b'}$ and $\boldsymbol{f}'_{i,b}$ according to to their subscripted index sets: $\{i, b'\}$ denotes the realisations of all input variables except that indexed by b in the i-th sample of $\boldsymbol{f}$ and $\{i, b\}$ denotes the realisation of the input variable indexed by b in the i-th sample of $\boldsymbol{f}'$.

Algorithm 1 Computing normalised estimated total-order Sobol' indices for n_B input variables.

procedure ComputeTotalSobolIndices(n_B)
Assign each input variable f_b an appropriate distribution
Sample N vectors, denoted $\boldsymbol{f_i}$, of size n_B by sampling each input variable f_b independently
Sample N vectors, denoted $\boldsymbol{f_i'}$, of size n_B by sampling each input variable f_b independently
for $b = 1, ..., n_B$ **do**
$\hat{\tilde{\tau}}_b^2 \leftarrow 0$
for $i = 1, ..., N$ **do**
$\hat{\tilde{\tau}}_b^2 += (g(\boldsymbol{f}_i) - g(\boldsymbol{f}_{i,b'} : \boldsymbol{f}'_{i,b}))^2$
$\hat{\tilde{\tau}}_b^2 \leftarrow \frac{\hat{\tilde{\tau}}_b^2}{2N}$
$\hat{\overline{S}}_b^2 \leftarrow \frac{\hat{\tilde{\tau}}_b^2}{\hat{\sigma}^2}$ ▷ This is the normalised total-order Sobol' index of input variable f_b.
return $\hat{\overline{\boldsymbol{S}}}^2$ ▷ This is a vector of n_B elements in which the b^{th} element is $\hat{\overline{S}}_b^2$.

$$\hat{\tilde{\tau}}_b^2 = \frac{1}{2N} \sum_{i=1}^{N} (g(\boldsymbol{f}_i) - g(\boldsymbol{f}_{i,b'} : \boldsymbol{f}'_{i,b}))^2 \tag{4}$$

Equation (5) gives the estimate of the normalised total-order Sobol' index for an input variable f_b, obtained by dividing the unnormalised estimate by the sample variance $\hat{\sigma}^2$, as given in Equation (6). Equation (7) computes the sample mean, needed in Equation (6).

$$\hat{\overline{S}}_b^2 = \frac{\hat{\tilde{\tau}}_b^2}{\hat{\sigma}^2} \tag{5}$$

$$\hat{\sigma}^2 = \frac{1}{N-1} \sum_{i=1}^{N} (g(\boldsymbol{f}_i) - \hat{\mu})^2 \tag{6}$$

$$\hat{\mu} = \frac{1}{N} \sum_{i=1}^{N} g(\boldsymbol{f}_i) \tag{7}$$

3.3 Bridge retrofit prioritization as a sensitivity analysis problem

Given a set of n_B bridges and a limited number of retrofits $R < n_B$ to allocate among them, the objective is to retrofit the bridges whose improved performance results in the greatest improvement in the performance of the road network. This requires modeling both bridge seismic retrofit and road network performance, detailed in this section, and formulating the SA problem. The proposed method is agnostic to the particular measure of road network performance used, which should reflect the priorities of the analyst using the proposed method to inform a retrofit prioritisation policy. In this paper, the road network performance is measured by a cost C.

3.3.1 Ground-motion and damage maps

To characterise the regional seismic hazard to which the road network is subject, n_S earthquake scenarios are generated from a seismic source model that specifies the rates at which earthquakes of particular magnitudes, locations, and faulting types occur. For each earthquake scenario j, an empirical ground-motion prediction equation (GMPE) is used to model the ground-motion intensity at each location of interest b. A GMPE predicts the mean of the log ground-motion intensity ($\ln Y$) as well as the ground-motion intensity within- and between-event residual standard deviations. A typical GMPE is function of many inputs, including the moment magnitude of the earthquake scenario M_j, the closest horizontal distance from location b to the surface projection of the fault plane R_{bj}, and the average shear wave velocity down to 30 meters at the b^{th} location $V_{s30,b}$. For each of the n_S earthquake scenarios, m ground-motion intensity maps can be sampled by sampling m realisations of the spatially-correlated ground-motion intensity residual terms (see, e.g., Han and Davidson, 2012 for a survey of sampling methods). The set of $n_S \times m$ ground-motion intensity maps is indexed using n (i.e., $n = 1, \ldots, n_S \times m$). Given residuals, the total log ground-motion intensity at a bridge b in a particular scenario n can be computed per Equation (8),

$$\ln Y_{bn} = \overline{\ln Y(M_j, R_{bn}, V_{s30,b}, \ldots)} + \sigma_{bn}\epsilon_{bn} + \tau_n\eta_n \tag{8}$$

where σ_{bn} is the within-event residual standard deviation, ϵ_{bn} is the normalised within-event residual in $\ln Y$, τ_n is the between-event residual standard deviation, η_n is the normalised between-event residual in $\ln Y$, and the other parameters are as defined above. Both ϵ_{bn} and η_n are standard normal random variables. ϵ_{bn} represents location-to-location variability, and its vector can be modelled using a spatially-correlated multivariate normal distribution. η_n represents between-event variability, and its vector can be modelled using a standard univariate normal distribution. The result of this procedure is a set of $n_S \times m$ ground-motion intensity maps. The annual rate of occurrence for the n^{th} ground-motion intensity map is the original rate of occurrence of the associated earthquake scenario n_S, divided by m, since m ground-motion intensity maps are simulated per earthquake scenario.

Given a ground-motion intensity map, n_D damage maps are sampled. A damage map is a vector of n_B binary variables, each indicating whether a particular bridge b is damaged. The probability that a bridge experiences at least some level of damage given a particular ground-motion intensity can be quantified using the bridge's fragility function, as given in Equation (9),

$$P(DS_b \geq ds | Y_b = y) = \Phi\left(\frac{\ln \frac{y}{f_b}}{\beta_b}\right) \tag{9}$$

where Y_b denotes the ground-motion intensity at site b in ground-motion intensity map n, Φ is the standard normal cumulative distribution function, and f_b and β_b are the mean and standard deviation, respectively, of the $\ln Y_b$ value required to cause the damage state of interest ds to occur or be exceeded for the b^{th} bridge (Miller, 2014). In this work, values of β_b are constant, in line with the recommendations of Buckle (1994). Bridge damage results

in the partial or total closure of the roads carried by the damaged bridge. Further details of modeling bridge damage are given in Section 4.3.

3.3.2 Bridge seismic retrofit

The seismic retrofit of a bridge $b \in \{1, \ldots, n_B\}$ is modelled as an increase in the median of the fragility function, f_b, as shown in Figure 1. The effect of a retrofit is quantified by a scaling factor, $\omega_b \geq 1$, by which f_b is multiplied (as devised in e.g., Kim and Shinozuka, 2004; Padgett and DesRoches, 2009 and used in e.g., Dong et al., 2014). In Figure 1, $\omega_b = 1.25$, shifting the fragility curve to the right and reducing the probability of the bridge sustaining at least damage state ds at every level of ground-motion intensity. The magnitude of ω_b depends on the bridge characteristics and intervention and can be determined from the literature.

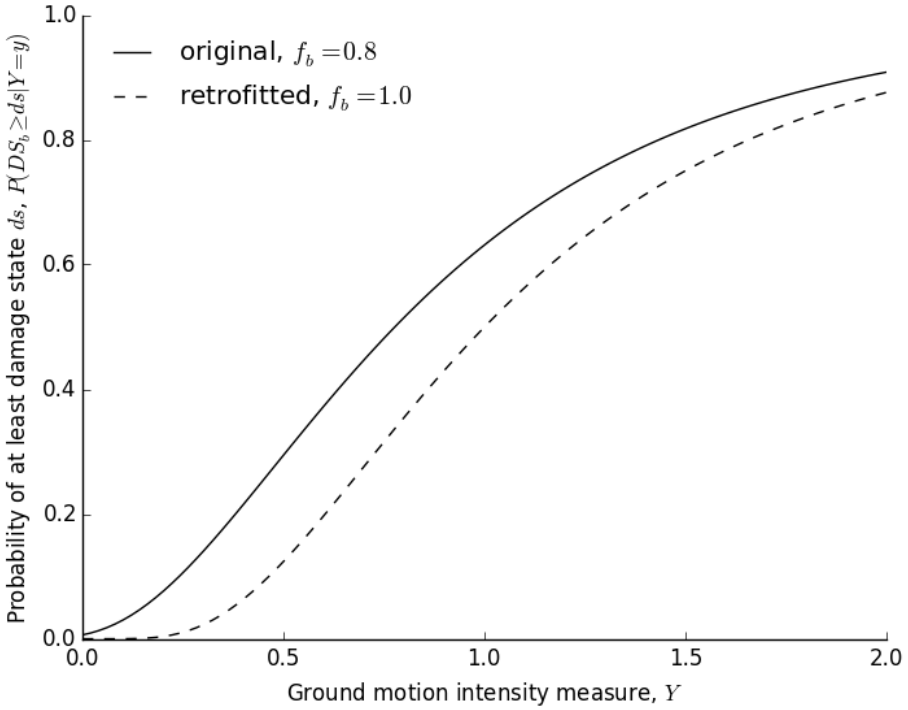

Figure 1: The fragility functions of a bridge with and without seismic retrofit, modelled as an increase in the median of the fragility function, f_b, with $\beta_b = 0.6$ before and after retrofit.

The seismic retrofit of a bridge b could be modelled more generally as a change in its state as defined by both the median and dispersion of its fragility curve, (f_b, β_b), without increasing the complexity of Algorithm 1. Padgett and DesRoches (2009) note, "Shifts in the median value are often indications of the most notable changes in vulnerability." An analyst implementing the proposed method should consider whether modeling changes in dispersion as a result of retrofit is appropriate for their particular use case.

3.3.3 Costs of road network performance

Disruptions to a road network can result in direct and indirect costs. Direct costs are those associated with restoring damaged road network components to their original states (Dong et al., 2014; Hackl et al., 2018). In addition to repairing damage from ground-shaking, restoration may be necessary to rehabilitate aging bridges or to repair damage due to traffic accidents, and including these costs is important when performing life-cycle analyses or coupling the proposed method with life-cycle costs (Decò & Frangopol, 2013). Restoring all network components to full functionality takes time t, during which the network will experience some level of disruption relative to its undamaged state (e.g., Kiremidjian et al., 2007). These ongoing disruptions can result in various indirect costs, including travel delays (due to congestion or rerouting) relative to the undamaged road network and connectivity losses, which occur when destinations that were reachable on the undamaged network become unreachable on the network with damaged components (Hackl et al., 2018). Other indirect costs include those associated with operating the road network, casualties, and environmental impacts such as carbon dioxide emissions and energy waste (Decò & Frangopol, 2013; Dong et al., 2014). Whichever sources of indirect cost considered, translating these network-level impacts of bridge damage to monetary units allows the consideration of multiple modes of loss at once. For each of the $n_S \times m$ ground-motion intensity maps considered, n_D damage maps are sampled, over which the average cost of the road network performance is computed for that particular ground-motion intensity map. The expected cost of the road network performance, $\mathbb{E}[C]$, can then be computed as the weighted average of the average cost associated with each ground-motion intensity map. The example of Section 4 includes the details of implementing a simple cost model; the proposed method is agnostic to the particular cost model used.

3.3.4 Sensitivity analysis problem formulation

The bridge retrofit problem is formulated as the SA problem in Equation (10),

$$\boldsymbol{f} \rightarrow \hat{\Psi}(\boldsymbol{f}) \rightarrow \mathbb{E}_{\mathcal{S}}[C(\boldsymbol{f})] \tag{10}$$

where $\boldsymbol{f} \in \mathbb{R}^{n_B}$ is a vector in which each element is f_b, the median of the fragility function of bridge $b \in \{1, \ldots, n_B\}$ that is associated with the damage state of interest, and $\hat{\Psi}(\boldsymbol{f})$ is a function that approximates $\mathbb{E}_{\mathcal{S}}[C(\boldsymbol{f})]$, the expected cost of the road network performance given bridge fragilities $\boldsymbol{f}$ and a set of ground-motion intensity maps, denoted $\mathcal{S}$, as in Equation (11),

$$\hat{\Psi}(\boldsymbol{f}_i) = \sum_{j=1}^{n_S} w_j \frac{1}{n_D} \sum_{k=1}^{n_D} C(D_{jk}(\boldsymbol{f}_i)) \tag{11}$$

where $\boldsymbol{f}_i$ is the i-th sample (vector) of bridge fragility function parameters, n_S is the number of ground-motion intensity maps in $\mathcal{S}$ (i.e., $m = 1$ ground-motion intensity map per earthquake scenario), w_j is the annual probability (or weight) of the ground-motion intensity map j, n_D is the number of damage maps per ground-motion intensity map, D_{jk} is the k-th realisation of the damage map sampled from ground-motion intensity map j, and $C()$ is the cost model. The cost with no bridge damage is 0, and therefore not included

in Equation (11). In this formulation, the total-order Sobol' index $\hat{\overline{\tau}}_b^2$ of a bridge's fragility function parameter f_b quantifies how much its variance contributes to the variance in the expected total cost of the road network's performance. The larger a bridge's total-order Sobol' index, the more influence its fragility has on the expected total cost of the road network's performance. To identify the bridges whose retrofit results in the greatest improvement in the road network's performance, the total-order Sobol' index $\hat{\overline{\tau}}_b^2$ of every bridge is estimated.

As described in Section 3.1, $\hat{\overline{\tau}}_b^2$ includes the interactions, of all orders, of the bridge's fragility function parameter with those of all other bridges in the group of bridges under study. The inclusion of these interactions between bridges' fragilities preserves the networked nature of this problem, i.e., that the bridges are part of a larger road network whose performance depends non-linearly and non-additively on their fragilities.

Using N samples of the fragility function parameter vector $\boldsymbol{f}$, the total-order Sobol' index $\hat{\overline{\tau}}_b^2$ of each bridge $b \in \{1, \ldots, n_B\}$ is estimated using Equation (4), where $i \in \{1, \ldots, N\}$ indexes the sample of $\boldsymbol{f}$ and the generic function $g()$ is replaced with our approximation of the expected cost, $\hat{\Psi}()$ (Sobol, 1993). To facilitate the comparison of bridges' total-order Sobol' indices, their normalised values, $\hat{\overline{S}}_b^2$, are reported using Equations (5) through (7). There are three prerequisites for setting up the SA problem in Equation (10) such that Sobol' indices can be computed.

1. The input variables f_b are independent.
2. The distribution of each input variable f_b is known (i.e., can be sampled from).
3. The output quantity of interest $\mathbb{E}_{\mathcal{S}}[C(\boldsymbol{f})]$ is a deterministic function of the input $\boldsymbol{f}$.

With respect to Prerequisite 1, bridge fragilities are assumed to be independent of one another. Because of Prerequisite 1, no retrofit budget can be imposed as a constraint when computing Sobol' indices – doing so would make bridges' fragility function parameters dependent. With respect to Prerequisite 2, the fragility function parameter f_b of each bridge is modelled as a binomial random variable with equal probabilities of being unretrofitted and retrofitted. With respect to Prerequisite 3, given a fixed set of ground-motion intensity maps and a fixed seed for damage simulation, $\mathbb{E}_{\mathcal{S}}[C(\boldsymbol{f})]$ is deterministic.

Once the total-order Sobol' indices of a set of n_B bridges have been estimated following Algorithm 1, with the function $\hat{\Psi}(\boldsymbol{f})$ replacing $g(\boldsymbol{f})$, the bridges are ranked in decreasing order of importance. This SA will be valid for the given set of ground-motion intensity maps; Section 4 will involve testing whether the resulting ranking is stable over other sets of ground-motion intensity maps.

4 Illustrative example

Each step in the proposed method is demonstrated on $n_B = 71$ state-owned highway bridges in San Francisco. Results are presented for the expected total cost of the road network performance ($\mathbb{E}[C]$), and a strategy for incorporating retrofit costs is demonstrated. The

particular models used and assumptions made in this example are not necessary to apply the proposed method; an analyst implementing the proposed method should select models and make assumptions appropriate for their particular use case.

4.1 Ground motion and damage maps

A set of 1992 ground-motion intensity maps is generated using the OpenSHA Event Set Calculator. As described in Section 3.3.1, each map comprises spatially correlated ground-motion intensities at all $n_B = 71$ bridge sites of interest and has an associated rupture scenario and annual occurrence rate (Miller, 2014). The ground-motion intensity measure for these maps is the 5%-damped pseudo absolute spectral acceleration (Sa) at a period of 1 second, the required input to the bridge fragility functions provided by Caltrans (Miller, 2014). Settings for the OpenSHA Event Set calculator were the Second Uniform California Earthquake Rupture Forecast (UCERF2) as the seismic source model, the Boore and Atkinson ground-motion prediction equation (Boore & Atkinson, 2008), and Wald and Allen's topographic slope model for the the shear wave velocity, V_{s30} (Miller, 2014).

To reduce computational expense, a subset of 30 ground-motion intensity maps, denoted $\mathcal{S}_1$, is initially selected from the set of 1992 ground-motion intensity maps using an optimisation method that minimises the difference between the annual exceedance curves of $\mathcal{S}_1$ and the full set of maps (Miller & Baker, 2013). The total-order Sobol' indices of each bridge in the set of interest are estimated using $\mathcal{S}_1$ according to Algorithm 1. Another subset of 45 ground-motion intensity maps $\mathcal{S}_2$ is then selected from the same portfolio of ground-motion maps using the same optimisation method and settings used to produce $\mathcal{S}_1$. $\mathcal{S}_2$ contains 19 maps also included in $\mathcal{S}_1$, though they are weighted differently (i.e., have different annual occurrence rates w_j) in each set. $\mathcal{S}_2$ is used to test (1) the performance of various bridge retrofit selection strategies and (2) whether bridge Sobol' indices computed on a smaller set of scenarios ($\mathcal{S}_1$) result in good performance on a larger set of scenarios. Both $\mathcal{S}_1$ and $\mathcal{S}_2$ produce the same ground-motion hazard at selected locations and the same distribution of numbers of damaged bridges – within a user-defined tolerance – as would the full set of maps, and are therefore hazard-consistent (Miller & Baker, 2013).

In this example, f_b is the median of the fragility function associated with the extensive damage state of bridge b; values of f_b were provided by Caltrans (Miller, 2014). Extensive bridge damage necessitates complete closure of the carried road and any associated underpasses, which are modelled as modifications of edge properties in the graph of the road network as detailed in Section 4.3.2. For this example, bridges not in the set of interest are considered invulnerable, an assumption not necessary to implement the proposed method.

4.2 Bridge seismic retrofit

The parameter ω is chosen according to each bridge's structural class, taking values ranging from $\omega = 1.17$ to $\omega = 1.33$ from Padgett and DesRoches (2009). While these values are associated with particular structural interventions (such as installing steel restrainer cables or column jackets), here they are taken as illustrative values only, for the purpose of demonstrating the proposed method.

4.3 Cost of road network performance

As shown in Equation (12), the cost of road network performance C is modelled as a function of C_{direct}, the costs associated with repairing damaged bridges, $C_{indirect}$, the costs associated with delays and unsatisfied travel demand, and t, the time period over which damage and the resulting drop in network performance persist (Hackl et al., 2018). The specification of this model's parameters is described here for a single damage map. The traffic and cost model used in this example is relatively simple. More sophisticated models might include variable demand on the road network after an earthquake (e.g., Feng et al., 2020) or more detailed modelling of road network restoration after an earthquake.

$$C = C_{direct} + t \times C_{indirect} \tag{12}$$

4.3.1 Direct costs

The direct cost, C_{direct}, is the sum of the repair costs of all the bridges in the road network for a given damage map.

$$C_{direct} = \sum_{b=1}^{B} C_{direct}^{(b)} \tag{13}$$

The direct cost associated with bridge b is computed per Equation (14),

$$C_{direct}^{(b)} = \mathbb{1}^{(b)} \times RCR \times A_b \times \text{ unit replacement cost} \tag{14}$$

where $\mathbb{1}^{(b)}$ is an indicator function that evaluates to 1 if bridge b is damaged and 0 otherwise, RCR is the mean repair cost ratio associated with the extensive damage state, and A_b denotes the area of bridge b. The product of the latter two terms in Equation (14) is the replacement cost of bridge b. In this example, the unit replacement cost of a bridge is 293 USD per square foot, or 3153.8 USD per square meter (*Recording and Coding Guide for the Structure Inventory and Appraisal of the Nation's Bridges*, 1995). An analyst who wished to incorporate more detailed information on the replacement costs of particular bridges could do so by modifying the latter two terms of Equation 14).

4.3.2 Indirect costs

The indirect cost of the road network performance, $C_{indirect}$, is modelled as a function of delays and unsatisfied travel demand for a given damage map. Aggregate travel time T and unsatisfied demand U are estimated on both undamaged and damaged versions of the road network using a graph of the road network, the demand on the road network, and an iterative traffic assignment (ITA) algorithm. The San Francisco Bay Area road network is modelled as a directed graph $G = (V, E)$: V comprises $11,958$ vertices representing road intersections and E comprises $33,005$ edges representing road links (Miller, 2014). The graph also includes 34 dummy nodes representing the centroids of travel superdistricts specified by the San Francisco Metropolitan Transportation Commission's travel model (Erhardt et al., 2012). The dummy nodes are used as the origins and destinations for the ITA algorithm. Each dummy node is connected to at least one real node and one real edge (Miller, 2014). Each edge in E has properties that determine its traversal time given a

traffic volume according to the Bureau of Public Roads travel time function,

$$t_a = t_f \left(1 + 0.15 \left(\frac{q_a}{c_f}\right)^4\right) \tag{15}$$

where t_f is the free-flow travel time, t_a is the capacity-dependent travel time, c_f is the hourly capacity, and q_a is the hourly flow on the edge (Bureau of Public Roads, 1964). All bridges in the road network are associated with edges in E. To model a complete road closure due to a damaged bridge, the associated edges are modified to have an hourly capacity $c_f = 0$ and both free-flow and capacity-dependent travel times $t_f, t_a = \infty$ to ensure no trips use those edges.

The daily demand on the road network is defined using the Bay Area Household Travel Survey of 2000 (International, 2000). In this example, the demand is fixed, i.e., invariant before and after an earthquake. The edge capacities of the links in G are hourly; the daily demand is scaled by a factor of 0.053 to get the hourly demand during the 6 am - 10 am window (Miller, 2014; Wang et al., 2012). Using an ITA algorithm, about $580,000$ trips are assigned to the road network between the 1156 OD pairs throughout the region. These trips represent the demand on the road network during one hour of the 6am - 10am peak travel window. The ITA algorithm divides the demand into four parts containing 40%, 30%, 20%, and 10% of the total trips. It assigns the first 40% of the trips to the shortest path, in terms of the sum of the traversed edges' free-flow travel times t_f, between the origin and destination. The shortest path is found using Djikstra's algorithm. The link flows q_a are updated to reflect the assigned trips, and the capacity-dependent travel times t_a are updated according to Equation (15). The ITA algorithm then assigns each remaining portion of the demand in a similar fashion; at each iteration, the edge weights considered by Djikstra's shortest path algorithm are t_a rather than t_f, reflecting congestion already on the road network.

For a given damage map, the costs associated with delays, C_{delays}, and those associated with unsatisfied demand, $C_{connectivity}$, are summed to get the indirect cost of the road network performance per Equation (16) (Hackl et al., 2018).

$$C_{indirect} = C_{delays} + C_{connectivity} \tag{16}$$

$$= \alpha \times \Delta T + \gamma \times \Delta U \tag{17}$$

where α is the value of time, γ is labor productivity, ΔT is the increase in travel time, and ΔU is the increase in unsatisfied demand; both ΔT and ΔU are computed relative to the undamaged network.

The parameters α and γ vary regionally and are estimated here for the San Francisco Bay Area. In this example, the demand on the road network as surveyed in 2000 is used as an input to the travel model; therefore, economic data from the year closest to 2000 is used to compute α and γ – that year is 2007, the first year for which state-level gross regional product information is available from the United States Bureau of Labor Statistics. For

the San Francisco Bay Area, the median household income in 2007 was 100,118.38 in 2020 dollars (Metropolitan Transportation Commission, 2019), resulting per Equation (18) in a value of travel time $\alpha = 48$ USD per hour of delay (Belenky, 2011).

$$\alpha = \frac{\text{median household income, USD}}{\text{2080 hours worked per year}} \tag{18}$$

The gross regional product of California in 2007 was 1,955,856 million USD in 2020 dollars while the number of labor hours in 2007 was 25,101 million (Pabilonia et al., 2019), resulting per Equation (19) in $\gamma = 78$ USD per hour per lost trip.

$$\gamma = \frac{\text{Annual gross regional product of California}}{\text{Annual labor hours in California}} \tag{19}$$

When a commuter cannot make a trip due to damage on the road network, it is assumed that they miss an 8-hour work-day. Commuters are assumed to have a five-day (40 hour) work week, and all trips considered during the one hour modelled are assumed to be commutes. Delays and connectivity losses for the single hour of demand assigned to the road network are assumed to persist throughout the day.

A restoration time of $t = 125$ days for an extensively damaged bridge is used per Shinozuka et al. (2003). The hourly indirect costs from Equation (16) are therefore multiplied by 125 days and 24 hours per day to get Equation (20).

$$C_{indirect} = 125 \text{ days} \times 24\frac{\text{hours}}{\text{day}} \times (C_{delays} + C_{connectivity}) \tag{20}$$

Assuming that demand during a peak commuting window persists throughout the day, that all trips in that window are commutes, and that the road network is not restored before 125 days almost certainly results in an over-estimate of indirect losses in this example.

4.4 Results: total-order Sobol' indices

Using Algorithm 1, each bridge's total-order Sobol' index with respect to $\mathbb{E}[C]$ is estimated using $N = 370$ samples of the fragility function parameter vector $\boldsymbol{f}$ and the smaller set of ground-motion maps $\mathcal{S}_1$, with $n_D = 10$ damage maps per ground-motion map. Table 1 lists the normalised estimated total-order Sobol' indices of the 10 most influential bridges, and Figure 2 shows their locations.

4.5 Results: testing retrofit strategies

For comparison with the results of the proposed method, bridges are ranked according to five other heuristic retrofit strategies. To get the composite ranking of a bridge, bridges are first ranked according to their *age* (from oldest to youngest), *fragility* function parameter f_b (from least to greatest), and daily average *traffic volume* (from most to least busy). The ranking of each bridge (ranging from 1 to 71) according to each of these characteristics is then summed to get a *composite* score; the bridges with the smallest *composite* scores are the most important. The retrofit strategy referred to as one-at-a-time (OAT) analysis is the only retrofit strategy besides the total-order Sobol' index-based strategy that takes

Ranking	$\hat{\overline{S}}_b^2$, $\mathbb{E}[C]$
1	0.707
2	0.087
3	0.062
4	0.027
5	0.027
6	0.026
7	0.017
8	0.007
9	0.006
10	0.004
...	...
Σ	0.97

Table 1: The 10 most influential bridges with respect to the expected total cost of the road network performance, $\mathbb{E}[C]$, and their normalised estimated total-order Sobol' indices based on $N = 370$ samples.

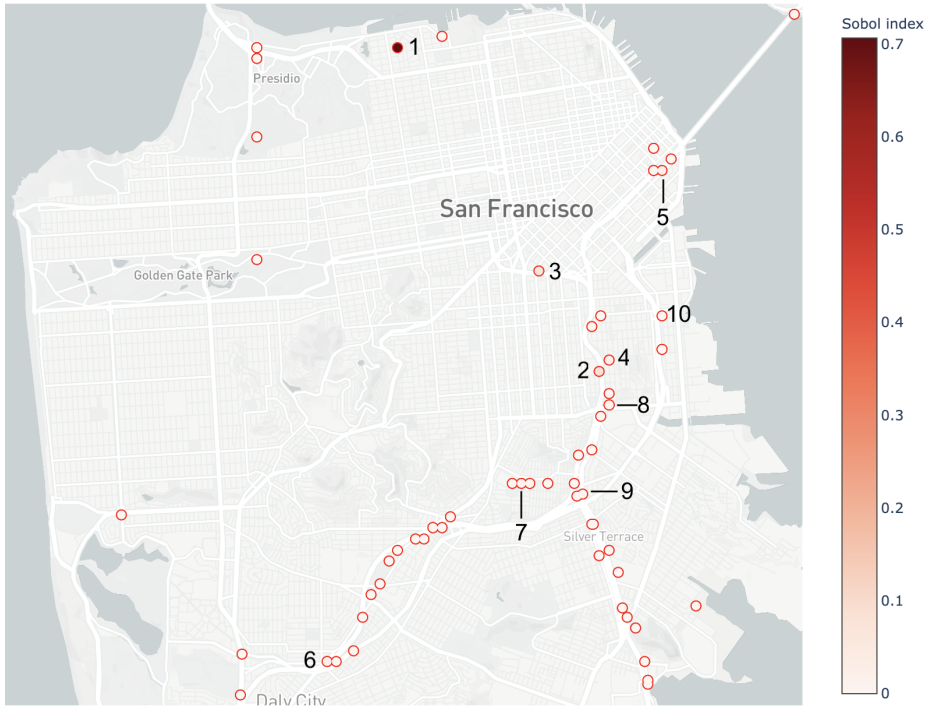

Figure 2: A map showing bridge locations and the relative magnitudes of their estimated total-order Sobol' indices, with respect to the expected total cost of the road network performance ($\mathbb{E}[C]$), based on $N = 370$ samples.

into account the performance of the road network to prioritise bridges. OAT analysis is a classic local (deterministic) sensitivity analysis technique, often used for networks, in which

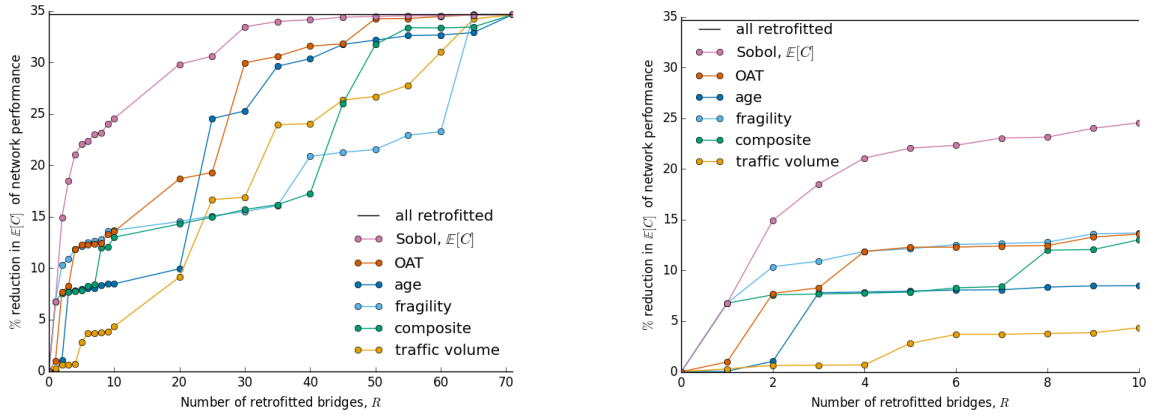

(a) (b)

Figure 3: Reduction in the expected total cost of the road network performance, $\mathbb{E}[C]$, given varying numbers of bridges retrofitted according to different prioritisation strategies. (a) Results for $R \leq 71$. (b) Results for $R \leq 10$.

the performance of the network when a single component is damaged is assessed for each component in the network (Borgonovo & Plischke, 2016). The components are then ranked according to the reduction in network performance that occurs when they are individually damaged.

Figure 3a shows the percent reduction in $\mathbb{E}[C]$ as a function of R, the number of bridges retrofitted. Expected cost is computed using the testing set, $\mathcal{S}_2$, to ensure that the results are not due to over-fitting. The performance of each retrofit strategy is bounded by the percent reduction in $\mathbb{E}[C]$ when $R = 0$ (0%) and when $R = n_B$ (34.6%). At every value of R, the retrofit strategy based on bridges' total-order Sobol' indices (henceforth referred to as the Sobol' strategy) produces the largest reduction in expected cost. The amount by which the Sobol' strategy outperforms the next best strategy is particularly striking in Figure 3a from $R = 2$ to $R = 50$. Figure 3b shows the percent reduction in $\mathbb{E}[C]$ for just $R \leq 10$. The gap between the Sobol' strategy and the next-best method is almost 5% at $R = 2$ and grows to more than 10% at $R = 10$, at which point the 10 retrofits selected by the Sobol' strategy account for almost 71% of the total reduction in the expected cost of the road network performance that can be achieved by retrofitting all bridges.

Figure 4 shows exceedance curves for the total cost of the road network performance, C, when $R = 8$ bridges are retrofitted according to each of the six retrofit strategies tested. For each strategy shown, the annual rate of exceedance, λ, of the cost (or loss) is computed using Equation (21),

$$\lambda = \sum_{j=1}^{n_S} w_j \frac{1}{n_D} \sum_{k=1}^{n_D} \mathbb{1}(C_{jk} \geq c) \tag{21}$$

where n_S is the number of ground-motion intensity maps in $\mathcal{S}_2$, w_j is the annual rate

of occurrence of the rupture associated with the ground-motion intensity map indexed by $j \in \{1, \ldots, n_S\}$, n_D is the number of damage maps sampled per ground-motion intensity map, and $\mathbb{1}()$ is an indicator function that evaluates to 1 if the cost C_{jk} associated with the k-th realisation of the damage map sampled from ground-motion intensity map j exceeds c, a cost threshold of interest, and to 0 otherwise. While the loss exceedance curve of the Sobol' strategy is comparable to those of the other retrofit prioritisation strategies at more frequent and lower-cost events, it performs much better than the other strategies at costs $> 2 \times 10^9$ USD, hewing closely to the curve associated with retrofitting all bridges. This suggests that the Sobol' strategy mitigates the more costly impacts of lower-probability events more effectively than the other retrofit strategies.

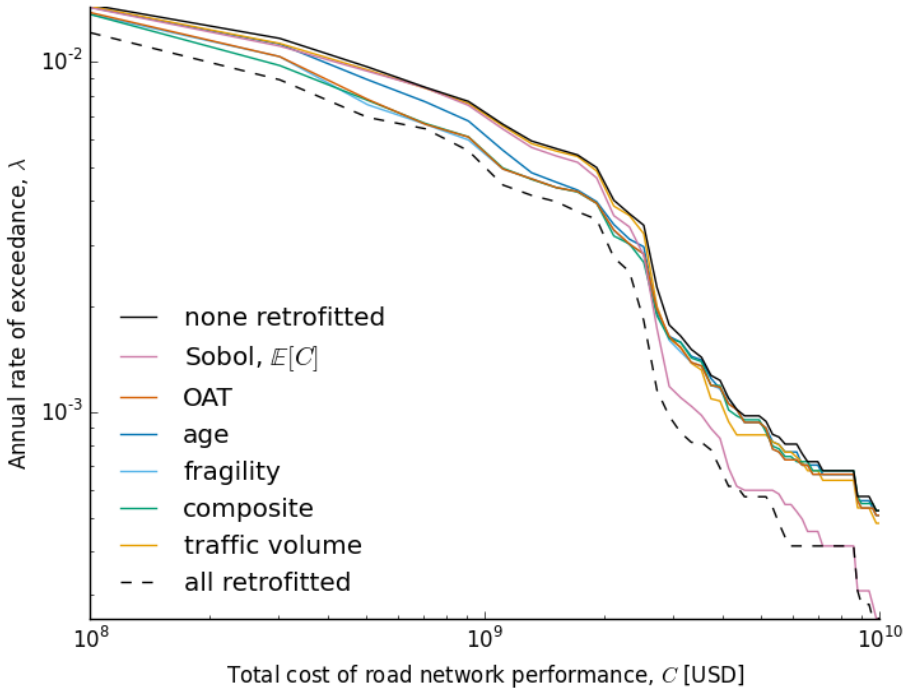

Figure 4: The annual rate of exceedance, λ, of the total cost of the road network performance, C, for $R = 8$ retrofits chosen according to six of the retrofit strategies tested.

4.6 Network effects

Figure 5 shows that the Sobol' strategy performs better than other strategies tested in part because it more quickly identifies network effects among bridges. A network effect occurs when the reduction in the expected total cost that occurs when two bridges are retrofitted is greater than the sum of the reductions that occur when each bridge is retrofitted separately (e.g., Saltelli et al., 2004). This is expressed mathematically in Equation (22), where R denotes the number of retrofits carried out, $\mathbb{E}[C|R = 0]$ denotes the expected cost of the road network performance when no retrofits have been carried out, $\mathbb{E}[C|\{r_1, \ldots, r_R\}]$ denotes the expected cost of the road network performance given a particular set of retrofits $\{r_1, \ldots, r_R\}$,

and $\mathbb{E}[C|r_n]$ denotes the expected cost of the road network performance given a single retrofit r_n.

$$\mathbb{E}[C|R=0] - \mathbb{E}[C|\{r_1, ..., r_R\}] > \sum_{n=1}^{R} (\mathbb{E}[C|R=0] - \mathbb{E}[C|r_n]) \tag{22}$$

Figure 5 plots Equation (23), the difference between the left- and right-hand sides of Equation (22) when expressed as percentages. A positive result of Equation (23) indicates a network effect. The Sobol' strategy achieves the maximum network effect of almost 3% at $R = 10$; the retrofit strategy based on bridges' ages is the next to attain the maximum network effect but does so only at $R = 23$. Other strategies never achieve the maximum network effect.

$$\text{network effect} = \left(\frac{\mathbb{E}[C|R=0] - \mathbb{E}[C|\{r_1, ..., r_R\}]}{\mathbb{E}[C|R=0]} - \sum_{n=1}^{R} \frac{(\mathbb{E}[C|R=0] - \mathbb{E}[C|r_n])}{\mathbb{E}[C|R=0]} \right) \times 100\% \tag{23}$$

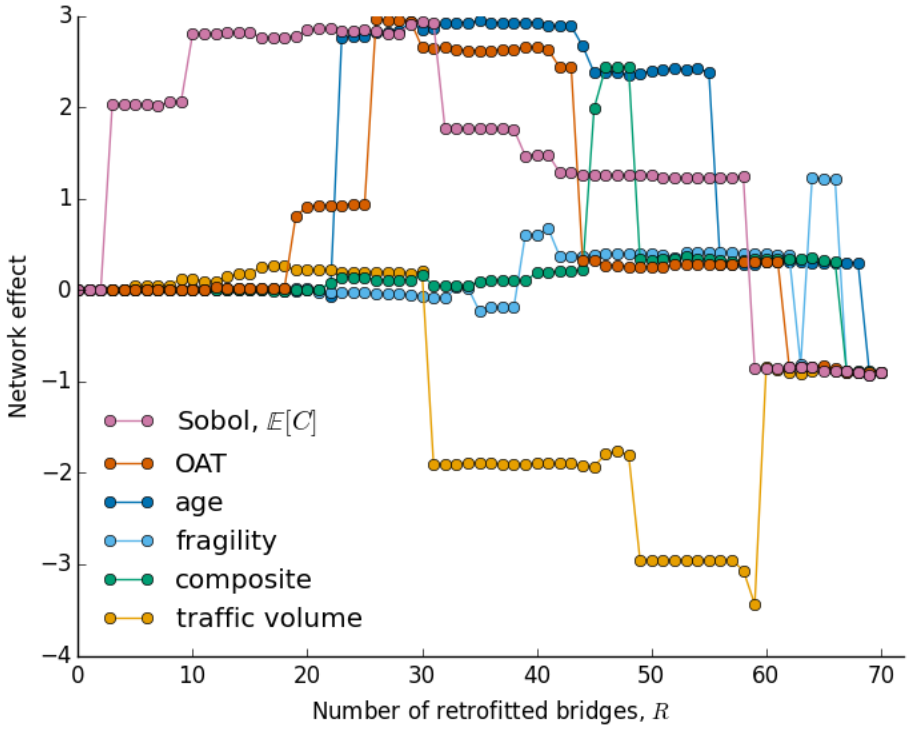

Figure 5: Network effects (as given by Equation (23) of bridge retrofits carried out according to six retrofit prioritisation strategies.

4.7 Accounting for retrofit costs

The proposed method does not allow for an explicit constraint on the total cost of bridge seismic retrofits as an optimisation problem might (e.g., Gomez & Baker, 2019). By changing the function whose sensitivity is being analysed, budgetary considerations can be incorporated into an analysis. To choose a set of retrofits that maximises the reduction in the expected cost of the road network performance per dollar spent on retrofits, Equation (24) can be used, where $C_R(\boldsymbol{f})$ denotes the cost of a set of retrofits described in $\boldsymbol{f}$.

$$\hat{\Psi}(\boldsymbol{f}) = \frac{\mathbb{E}[C]}{C_R(\boldsymbol{f})} \tag{24}$$

To implement Equation (24), it is assumed that retrofitting a bridge costs 25% as much as repairing it. Figure 6 shows that a strategy based on total-order Sobol' indices estimated with respect to Equation (24) outperforms the six other strategies tested. For just 13% of the cost of retrofitting all 71 bridges, the Sobol' cost-ratio-based strategy achieves 87.5% of the total reduction in the network performance cost that can be achieved by retrofitting bridges. That the Sobol' cost-ratio-based strategy performs so well is not surprising, since none of the other strategies can take into account the cost of retrofits, a commonly cited limitation of heuristic methods for retrofit prioritisation. Because the total-order Sobol' indices with respect to Equation (24) were estimated using the same set of $N = 370$ sample evaluations used to prioritise bridges with respect to $\mathbb{E}[C]$ in Sections 4.4 and 4.5, no additional simulations of road network performance were required.

5 Discussion

Implementing Algorithm 1 is straightforward; standard verification problems are well documented, e.g., estimating the Sobol' indices of the Ishigami function (Ishigami & Homma, 1990). This section discusses other practical considerations for using this method: its computational complexity, the number of samples required, and the effect of the binomial distribution parameter p.

5.1 Computational complexity

Evaluating $\hat{\Psi}(\boldsymbol{f}_i)$ requires sampling damage maps and simulating traffic on each damage map. Simulating traffic is much more computationally expensive than sampling damage maps. Therefore, knowing the number of traffic simulations required for a particular number of bridges, n_B, number of ground-motion maps, n_S, number of damage maps per ground-motion map, n_D, and number of samples of $\boldsymbol{f}$, N, is necessary to plan experiments. Equation (25) gives the number of function evaluations n_f required to compute the total-order Sobol' indices for each bridge in a set of n_B bridges for the function $\hat{\Psi}(\boldsymbol{f}_i) \approx \mathbb{E}_{\mathcal{S}}[C(\boldsymbol{f})]$ using Algorithm 1.

$$n_f = (N \times n_S \times n_D)(n_B + 1) \tag{25}$$

Though n_f may seem large, the Sobol' index method is well suited to parallelisation over samples of $\boldsymbol{f}$ because each sample is evaluated independently. As described in Section 4, if

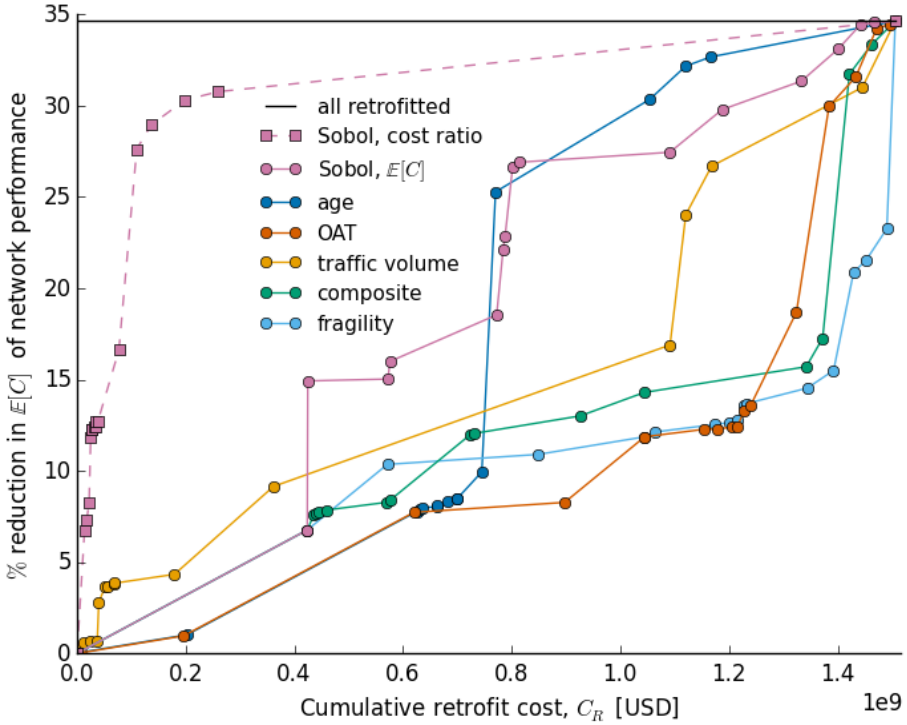

Figure 6: Reduction in the expected total cost of road network performance, $\mathbb{E}[C]$, versus the cost of retrofitting varying numbers of bridges according to different prioritisation strategies, one of which is the Sobol' index strategy based on Equation (24), which accounts for both the road network performance and the cost of retrofits.

multiple outputs of interest are stored from each sample evaluation, the same set of samples can be used to evaluate the sensitivities of each output.

5.2 Number of samples required

The number of samples required to estimate the Sobol' indices of a set of bridges is not evident *a priori*, in part because the criteria that define a satisfactory estimate vary by application. If the objective of a study is to develop a probabilistic ranking of bridges to retrofit, then one criterion might be that the ranking is a confident one, e.g., that the 95% confidence intervals of the bridges' sensitivity indices do not overlap. This may be difficult to achieve in practice. If the objective of a study is to select a limited number R of bridges to retrofit, a more achievable criterion might be that the 95% confidence intervals of the R and $R+1$ most influential bridges should not overlap.

Finding an appropriate sample size for an application will likely prove an iterative process and depend on available computational resources and objective, as it did in the case study, for which 370 samples were used as the basis for the Sobol' strategy. To investigate the goodness of the ranking established on the basis of that sample size, in this section

90 additional samples (an increase of about 25%) are used to estimate bridges' total-order Sobol' indices and establish a "final" ranking against which rankings based on smaller sample sizes can be compared.

Figure 7 shows the convergence of the total-order Sobol' indices (with respect to $\mathbb{E}[C]$) as a function of the sample size, N, for the bridges ranked 3rd through 7th most important. Figure 7 was produced using bootstrapping: at each value of $N \leq 460$, N samples of the fragility function parameter vector $\boldsymbol{f}$ that had been previously generated were randomly chosen (with replacement), on the basis of which bridges' total-order Sobol' indices were estimated according to Algorithm 1. At each N, the aforementioned step was repeated 100 times to estimate the mean, standard deviation, and 95% confidence interval of each bridge's total-order Sobol' index. Previous evaluations of $\boldsymbol{f}$ and associated hybrid points were used.

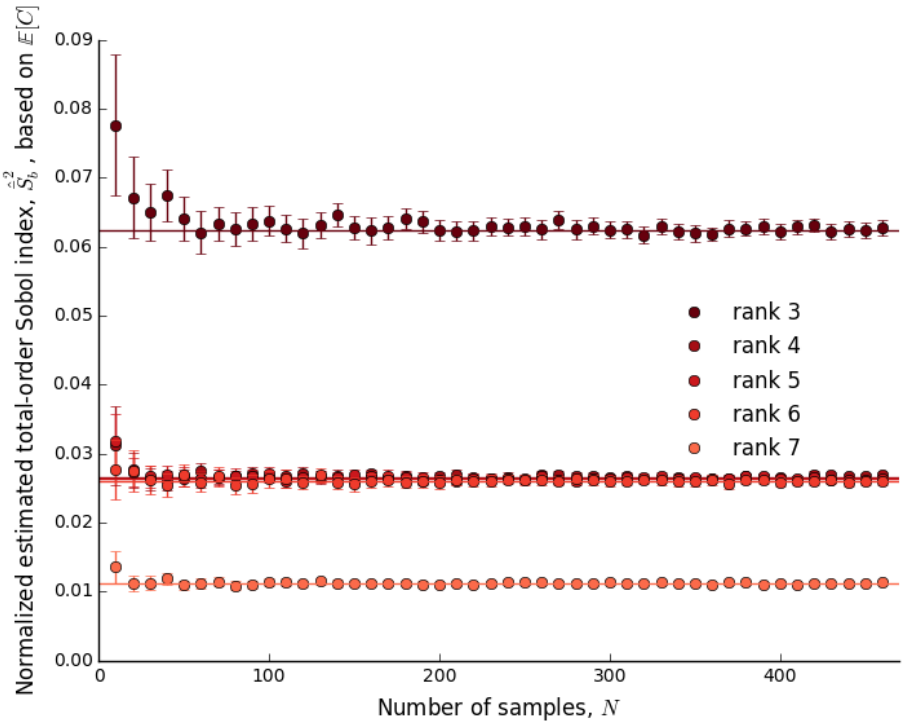

Figure 7: The convergence of the total-order Sobol' indices of the bridges ranked 3th through 7th most important with respect to the expected total cost of road network performance ($\mathbb{E}[C]$) computed over $\mathcal{S}_1$. Whiskers indicate 95% confidence intervals.

While the relative importance of the 3rd and 7th most important bridges in Figure 7 is clear even at $N = 10$, the 95% confidence intervals of the 4th, 5th, and 6th ranked bridges overlap even at the maximum $N = 460$. If our objective were to select $R = 4$ bridges to retrofit, this result would be less than ideal. The similarity of the three bridges' total-order Sobol' indices may indicate that selecting any one of them as the fourth retrofit would have a

similar effect on $\mathbb{E}[C]$ – however, that cannot be inferred from their total-order indices alone. Let b_4, b_5, and b_6 denote the three bridges with similar total-order Sobol' indices as ranked using $N = 460$ samples (i.e., without bootstrapping). To know which bridge would have the greatest effect on $\mathbb{E}_C$ as the fourth retrofit, each bridge's fourth-order sensitivity index with respect to the three bridges already selected for retrofit would have to be estimated. In lieu of that inconvenient computation, these three bridges can instead be ranked in decreasing order of their estimated first-order Sobol' indices (per Sobol, 1993 and using 370 samples): b_6, b_5, b_4. Because b_6 has a larger first-order Sobol' index than the other two bridges but a similar total-order index, retrofitting b_6 fourth would be expected to reduce $\mathbb{E}[C]$ more than retrofitting b_4 or b_5. This result is evident in Figure 8, which shows the performance of Sobol' index-based retrofit strategies for $R \leq 10$ based on sample sizes of $N = 100, 150, 200, 300, 400$, and 460. At $R = 4$, the best-performing strategy chooses b_6, beating the other strategies by about 1.5%. At $R = 5$, the best-performing strategies choose b_6, beating the other strategy by about 2.25%. Whether estimating bridges' first-order Sobol' indices is warranted depends on the objective and the results of the total-order analysis – since the method developed by Sobol' for first-order index estimation requires evaluating different hybrid points than those used to estimate total-order Sobol' indices, the additional computational expense may be considerable (Sobol, 1993).

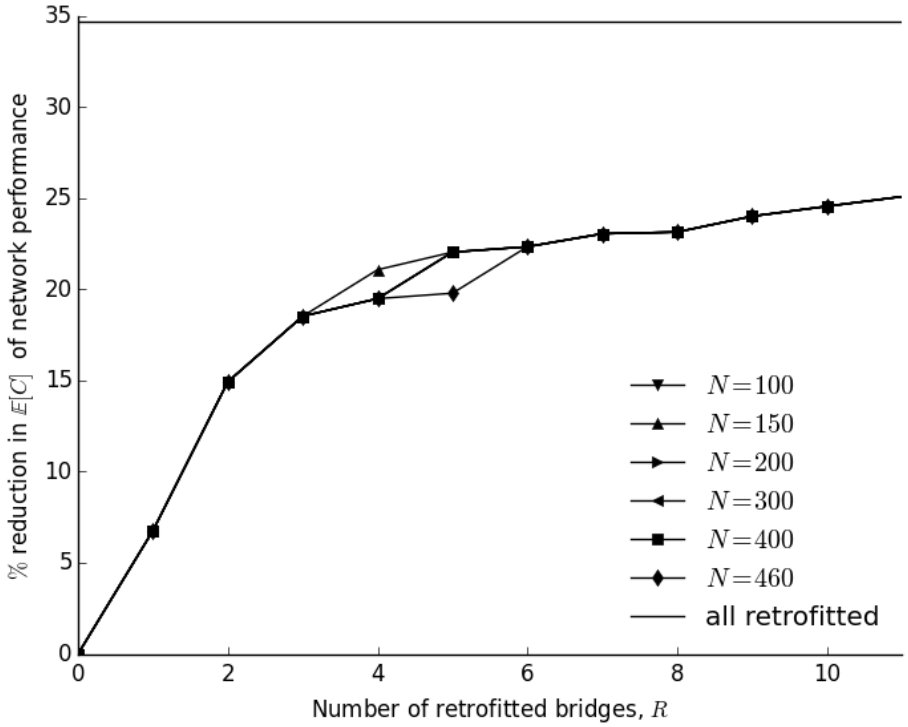

Figure 8: Reduction in $\mathbb{E}[C]$ as a function of the number of retrofits, R, with retrofits chosen using bridges' total-order Sobol' indices computed using different sample sizes, N.

Figures 9a and 9b show the convergence of the rankings of different subsets of the $B = 71$ bridges of interest with increasing N. The final rankings in both Figure 9a and 9b

are based on bridges' total-order Sobol' indices with respect to $\mathbb{E}[C]$ and estimated using $N = 460$ samples of $\boldsymbol{f}$. The subsets in Figure 9a are overlapping, while those in Figure 9b are disjoint. The y-axis of both figures plots the fraction of bridges in a particular subset whose rankings at a sample size $N < 460$ match their rankings using the full set of $N = 460$ samples; a value of 1 indicates that the ranking of every bridge in the subset matches its ranking using $N = 460$ samples.

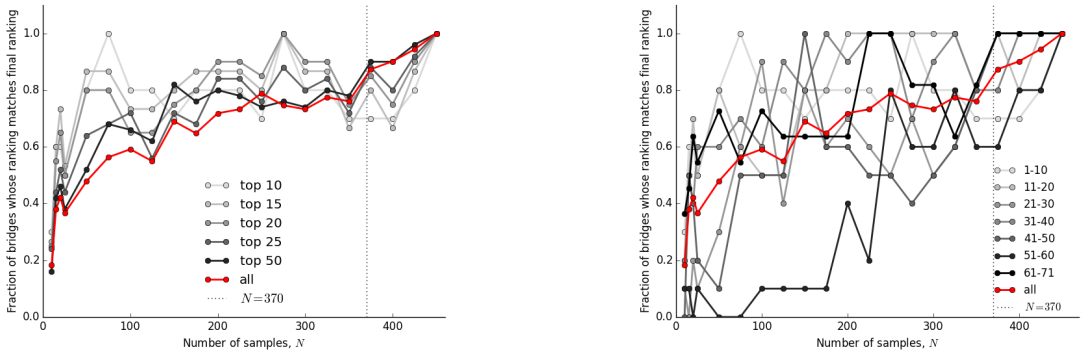

(a) (b)

Figure 9: The convergence of sets of bridges to their ranking using $N = 460$ samples with increasing sample size N. (a) Results for (overlapping) sets of the most important bridges. (b) Results for disjoint sets of 10 bridges.

In both Figures 9a and 9b, the convergence of subsets of bridges' rankings is noisy, though the convergence of the overall ranking (denoted "all") is generally increasing with N. This noisiness stems from two related factors: (1) the difficulty of estimating small Sobol' indices: at $N = 460$, the total-order Sobol' index of the 24th most important bridge is on the order of 10^{-5}, while that of the 70th most important bridge is on the order of 10^{-10} and (2) bridges with similarly valued total-order Sobol' indices (as in Figure 7) switching places in the rankings as N changes. With regard to (1), techniques exist for better estimating small Sobol' indices, using estimators other than the one described in Section 3 (Owen, 2013, e.g.,). For typical prioritisation applications, these may be unnecessary, since such small normalised total-order Sobol' indices indicate the retrofits are non-influential. With regard to (2), attempting to establish a confident ranking of bridges with similarly valued estimated total-order Sobol' indices may be worth the effort and additional computational expense if those bridges are not non-influential. In that case, using bootstrapping is an inexpensive way to initially investigate the accuracy of the estimated indices. Certain situations may call for the estimation of first-order Sobol' indices. However, if the magnitudes of the similarly-valued normalised total-order Sobol' indices are very small, further investigation will not improve the results of a particular retrofit prioritisation. Despite the apparent instability of the rankings shown in Figures 9a and 9b, the performance of bridge retrofit strategies based on different sample sizes shows notable discrepancies only at $R = 4$ and $R = 5$, as shown in Figure 8, and is identical at $R > 10$ (not shown).

5.3 Effect of binomial distribution parameter p

In Sections 3 and 4, each bridge's fragility function parameter f_b is modelled as a binomial random variable with equally probable ($p = 0.5$) outcomes of taking on unretrofitted and retrofitted values. The choice of $p = 0.5$ is not obvious. Therefore, three sets of $N = 190$ samples of the fragility vector $\boldsymbol{f}$ are constructed using binomial distributions with retrofit probabilities $p = 0.2$, $p = 0.5$, and $p = 0.8$. Bridges' total-order Sobol' indices are then estimated using each set of samples and the three resulting retrofit strategies tested. The three sets of indices produce nearly identical rankings, with only two small deviations that result from the finite sample sizes used for estimation. These discrepancies may be resolved with larger N. No one value of p consistently results in a better or worse retrofit prioritization.

5.4 Limitations of the proposed method

The proposed method does not guarantee an optimal set of bridge retrofits, nor can it take into account a retrofit budget, which is typically a constraint in real applications. Though different structural interventions can be considered for different bridges, the proposed method does not consider multiple levels of structural intervention for a single bridge. The proposed method is more computationally expensive than the other heuristic strategies tested in Section 4 because our function $\hat{\Psi}$ requires traffic simulation that accounts for the bulk ($> 99\%$) of the total runtime. Faster traffic simulation would dramatically reduce the computational cost of the proposed method; the actual number of samples required may be quite modest.

6 Conclusions

This paper (1) details a global sensitivity-analysis-based method for prioritising bridge seismic retrofits within a regional road network, (2) shows that the proposed method outperforms extant heuristic bridge retrofit prioritisation strategies in a case study of San Francisco, and (3) discusses practical considerations for using the proposed method for infrastructure management problems beyond our example.

The inputs of the SA problem are the medians of bridges' fragility functions for a damage state of interest and the output is a network performance metric of interest. Each bridge's fragility function median is modelled as an independent binary variable that takes values corresponding to unretrofitted and retrofitted states. The output is the expected cost of the road network performance over a set of ground-motion intensity maps $\mathcal{S}_1$, estimated using a probabilistic seismic risk assessment framework. The sensitivity of the expected cost to the retrofit status of each bridge is quantified by estimating bridges' total-order Sobol' indices using the hybrid-point Monte Carlo approximation technique developed by Sobol'. The greater a bridge's total-order Sobol' index, the more important retrofitting that bridge is to reduce the expected cost.

The proposed method is demonstrated on 71 unique bridges in the County of San

Francisco, considering a travel model for the nine-county Bay Area. The performance of a retrofit strategy based on bridges' total-order Sobol' indices is compared with that of five other heuristic retrofit prioritisation strategies by computing the reductions in the expected cost of network performance that result from retrofitting bridges over a larger set of ground-motion intensity maps, $\mathcal{S}_2$. The Sobol'-index-based strategy outperforms the other strategies in part because it identifies network effects between bridges. The computational cost of the proposed method is dominated by the number of traffic model evaluations required, which is a function of the seismic risk analysis parameters and the number of samples of bridges' fragility function medians. Because each input sample is evaluated independently, the proposed method is easily parallelised. For some applications, a small number of samples may suffice.

The proposed bridge retrofit prioritisation method remains computationally tractable while accounting for the probabilistic nature of the seismic hazard, the uniqueness of individual bridges, the link between road network performance and individual bridges' retrofit statuses, and network effects in terms of bridge damage and bridge retrofit. It can also incorporate budgetary considerations (though not constraints). Because this method leverages existing risk assessment tools and models without imposing further assumptions, it should be extensible to other types of networks under different types of hazards and with consideration given to different decision-makers' priorities.

Acknowledgements

This work was supported in part by the Shah Fellowship on Catastrophic Risk at Stanford University. The authors thank Zachary del Rosario, Sita Syal, and Andy Ziccarelli for their comments. Some of the computing for this project was performed on the Sherlock cluster. The authors thank Stanford University and the Stanford Research Computing Center for providing computational resources and support that contributed to these research results.

Data availability

The code and data that support the findings of this study are openly available in *Sobol' index-based bridge retrofit prioritisation code* at https://doi.org/10.5281/zenodo.4294322.

Declaration of interests

The authors have no conflicts of interest to disclose.

References

Barbarasoglu, G., & Arda, Y. (2004). A two-stage stochastic programming framework for transportation planning in disaster response. *Journal of the Operational Research Society*, *55*, 43–53. https://doi.org/10.1149/1.1697412

Barker, K., Ramirez-Marquez, J. E., & Rocco, C. M. (2013). Resilience-based network component importance measures. *Reliability Engineering and System Safety*, *117*, 89–97. https://doi.org/10.1016/j.ress.2013.03.012

Belenky, P. (2011). Revised departmental guidance on valuation of travel time in economic analysis. *Office of Transportation Policy Reports*, 1–28.

Boore, D. M., & Atkinson, G. M. (2008). Ground-motion prediction equations for the average horizontal component of pga, pgv, and 5%-damped psa at spectral periods between 0.01 s and 10.0 s. *Earthquake Spectra*, *24*(1), 99–138. https://doi.org/10.1193/1.2830434

Borgonovo, E., & Plischke, E. (2016). Sensitivity analysis: A review of recent advances. *European Journal of Operational Research*, *248*(3), 869–887. https://doi.org/10.1016/j.ejor.2015.06.032

Buckle, I. G. (1994). *The northridge california earthquake of january 17, 1994: Performance of highway bridges* (tech. rep.). National Center for Earthquake Engineering Research.

Buckle, I. G., Friedland, I., Mander, J., Martin, G., Nutt, R., & Power, M. (2006). *Seismic retrofitting manual for highway structures: Part 1 - bridges* (tech. rep.). Multidisciplinary Center for Earthquake Engineering Research.

Bureau of Public Roads. (1964). *Traffic assignment manual for application with a large, high speed computer.* (tech. rep.). U.S. Department of Commerce, Urban Planning Division. Washington, D.C.

Chang, L., Peng, F., Ouyang, Y., Elnashai, A. S., & Spencer, Jr., B. F. (2012). Bridge seismic retrofit program planning to maximize postearthquake transportation network capacity. *Structure and Infrastructure Engineering*, *18*, 75–88. https://doi.org/10.1061/(ASCE)IS

Decò, A., & Frangopol, D. M. (2013). Life-cycle risk assessment of spatially distributed aging bridges under seismic and traffic hazards. *Earthquake Spectra*, *29*(1), 127–153. https://doi.org/10.1193/1.4000094

Dong, Y., Frangopol, D. M., & Saydam, D. (2014). Pre-earthquake multi-objective probabilistic retrofit optimization of bridge networks based on sustainability. *Journal of Bridge Engineering*, *19*(6), 04014018. https://doi.org/10.1061/(ASCE)BE.1943-5592.0000586

Dutuit, Y., & Rauzy, A. (2015). On the extension of importance measures to complex components. *Reliability Engineering and System Safety*, *142*, 161–168. https://doi.org/10.1016/j.ress.2015.04.016

Erhardt, G., Ory, D., Sarvepalli, A., Freedman, J., Hood, J., & Stabler, B. (2012). Mtc 's travel model one: Applications of an activity-based model in its first year. *Innovations in Travel Modeling*, (9).

Fan, Y., Liu, C., Lee, R., & Kiremidjian, A. S. (2010). Highway network retrofit under seismic hazard. *Journal of Infrastructure Systems*, *16*(3), 181–187. https://doi.org/10.1061/?ASCE?IS.1943-555X.0000024

Feng, K., Li, Q., & Ellingwood, B. R. (2020). Post-earthquake modelling of transportation networks using an agent-based model. *Structure and Infrastructure Engineering*, *16*(11), 1578–1592. https://doi.org/10.1080/15732479.2020.1713170

Frangopol, D. M., & Bocchini, P. (2012). Bridge network performance, maintenance and optimisation under uncertainty: Accomplishments and challenges. *Structure and Infrastructure Engineering*, *8*(4), 341–356. https://doi.org/10.1080/15732479.2011.563089

Giovinazzi, S., Wilson, T., Davis, C., Bristow, D., Gallagher, M., Schofield, A., Villemure, M., Eidinger, J., & Tang, A. (2011). Lifelines performance and management following the 22 february 2011 christchurch earthquake, new zealand: Highlights of resilience. *Bulletin of the New Zealand Society for Earthquake Engineering*, *44*(4), 402–417. https://doi.org/10.5459/bnzsee.44.4.402-417

Gomez, C., & Baker, J. W. (2019). An optimization-based decision support framework for coupled pre- and post-earthquake infrastructure risk management. *Structural Safety*, *77*(October 2017), 1–9. https://doi.org/10.1016/j.strusafe.2018.10.002

Gordon, P., Richardson, H. W., & Davis, B. (1998). Transport-related impacts of the northridge earthquake. *Journal of Transportation and Statistics*, *1*(2), 21–36.

Grass, E., & Fischer, K. (2016). Two-stage stochastic programming in disaster management: A literature survey. *Surveys in Operations Research and Management Science*, *21*(2), 85–100. https://doi.org/10.1016/j.sorms.2016.11.002

Hackl, J., Adey, B. T., & Lethanh, N. (2018). Determination of near-optimal restoration programs for transportation networks following natural hazard events using simulated annealing. *Computer-Aided Civil and Infrastructure Engineering*, *33*(8), 618–637. https://doi.org/10.1111/mice.12346

Han, Y., & Davidson, R. A. (2012). Probabilistic seismic hazard analysis for spatially distributed infrastructure. *Earthquake Engineering & Structural Dynamics*, *41*, 2141–2158. https://doi.org/10.1002/eqe

International, M. (2000). Bay area travel survey. https://doi.org/10.3886/ICPSR34805.v1

Ishigami, T., & Homma, T. (1990). An importance quantification technique in uncertainty analysis for computer models. *First International Symposium on Uncertainty Modeling and Analysis*, 398–403.

Kim, S. H., & Shinozuka, M. (2004). Development of fragility curves of bridges retrofitted by column jacketing. *Probabilistic Engineering Mechanics*, *19*(1), 105–112. https://doi.org/10.1016/j.probengmech.2003.11.009

Kiremidjian, A. S., Stergiou, E., & Lee, R. (2007). Issues in seismic risk assessment of transportation networks. *Geotechnical, geological and earthquake engineering* (pp. 461–480). https://doi.org/10.1007/978-1-4020-5893-6_19

Liu, C., Fan, Y., & Ordóñez, F. (2009). A two-stage stochastic programming model for transportation network protection. *Computers and Operations Research*, *36*(5), 1582–1590. https://doi.org/10.1016/j.cor.2008.03.001

Liu, M., & Frangopol, D. M. (2005). Time-dependent bridge network reliability: Novel approach. *Journal of Structural Engineering*, *131*(2), 329–337. https://doi.org/10.1061/(ASCE)0733-9445(2005)131:2(329)

Metropolitan Transportation Commission. (2019). Bay area transportation study.

Miller, M. (2014). *Seismic risk assessment of complex transportation networks* (Doctoral dissertation). Stanford University.

Miller, M., & Baker, J. W. (2013). Ground-motion intensity and damage map selection for probabilistic infrastructure network risk assessment using optimization. *Earth-*

quake Engineering and Structural Dynamics, *00*, 1–20. https://doi.org/10.1002/eqeGround-motion

Miller-Hooks, E., Zhang, X., & Faturechi, R. (2012). Measuring and maximizing resilience of freight transportation networks. *Computers and Operations Research*, *39*(7), 1633–1643. https://doi.org/10.1016/j.cor.2011.09.017

Moghtaderi-Zadeh, M., & Kiureghian, A. D. (1983). Reliability upgrading of lifeline networks for post-earthquake serviceability. *Earthquake Engineering & Structural Dynamics*, *11*(4), 557–566. https://doi.org/10.1002/eqe.4290110408

Owen, A. B. (2013). Better estimation of small sobol' sensitivity indices. *ACM Transactions on Modeling and Computer Simulation*, *23*(2). https://doi.org/10.1145/2457459.2457460

Pabilonia, S., Jadoo, M., Khandrika, B., Price, J., & Mildenberger, J. (2019). Bls publishes experimental state-level labor productivity measures. *Monthly Labor Review*, (June), 1–25. https://doi.org/10.21916/mlr.2019.12

Padgett, J. E., & DesRoches, R. (2009). Retrofitted bridge fragility analysis for typical classes of multispan bridges. *Earthquake Spectra*, *25*(1), 117–141. https://doi.org/10.1193/1.3049405

Peeta, S., Sibel Salman, F., Gunnec, D., & Viswanath, K. (2010). Pre-disaster investment decisions for strengthening a highway network. *Computers and Operations Research*, *37*(10), 1708–1719. https://doi.org/10.1016/j.cor.2009.12.006

Recording and coding guide for the structure inventory and appraisal of the nation's bridges (tech. rep.). (1995). U.S. Department of Transportation Federal Highway Administration. Washington, D.C.

Rokneddin, K. (2013). *Reliability and risk assessment of networked urban infrastructure systems under natural hazards* (Doctoral dissertation). Rice University.

Rokneddin, K., Ghosh, J., Dueñas-Osorio, L., & Padgett, J. E. (2013). Bridge retrofit prioritisation for ageing transportation networks subject to seismic hazards. *Structure and Infrastructure Engineering*, *9*(10), 1050–1066. https://doi.org/10.1080/15732479.2011.654230

Saltelli, A., Ratto, M., Andres, T., Campolongo, F., Cariboni, J., Gatelli, D., Saisana, M., & Tarantola, S. (2008). *Global sensitivity analysis: The primer*. John Wiley; Sons, Ltd.

Saltelli, A., Tarantola, S., Campolongo, F., & Ratto, M. (2004). *Sensitivity analysis in practice: A guide to assessing scientific models* (Vol. 101). John Wiley; Sons, Ltd.

Shinozuka, M., Murachi, Y., Dong, X., Zhou, Y., & Orlikowski, M. J. (2003). Effect of seismic retrofit of bridges on transportation networks. *Earthquake Engineering and Engineering Vibration*, *2*(2), 169–179. https://doi.org/10.1007/s11803-003-0001-0

Sims, B. H. (2000). *On shifting ground : Earthquakes , retrofit and engineering culture in california* (Doctoral dissertation). University of California, San Diego.

Sobol, I. (1993). Sensitivity estimates for nonlinear mathematical models. *Mathematical Modelling and Computational Experiments*, (1), 407–414.

Song, J., & Kiureghian, A. D. (2005). Component importance measures by linear programming bounds on system reliability. *Proceedings of the 9th International Conference on Structural Safety and Reliability*.

Bhattacharjee, G., and Baker, J. W. (2023). "Using global variance-based sensitivity analysis to prioritise bridge retrofits in a regional road network subject to seismic hazard." *Structure and Infrastructure Engineering* 19(2), 164-177. https://doi.org/10.1080/15732479.2021.1931892

Wang, Q., Guan, Y., & Wang, J. (2012). A chance-constrained two-stage stochastic program for unit commitment with uncertain wind power output. *IEEE Transactions on Power Systems*, *27*(1), 206–215. https://doi.org/10.1109/TPWRS.2011.2159522

Zhang, W., & Wang, N. (2016). Resilience-based risk mitigation for road networks. *Structural Safety*, *62*, 57–65. https://doi.org/10.1016/j.strusafe.2016.06.003